Published in final edited form as:
Biochem Pharmacol. 2013 March 15; 85(6): 817–828. doi:10.1016/j.bcp.2013.01.010.

Point-to-point ligand-receptor interactions across the subunit interface modulate the induction and stabilization of conformational states of alpha7 nAChR by benzylidene anabaseines[1]

Matthew D. Isaacson[a,2], **Nicole A. Horenstein**[b], **Clare Stokes**[c], **William R. Kem**[d], and **Roger L. Papke**[e]

[a]Department of Pharmacology and Therapeutics, University of Florida College of Medicine, P.O. Box 100267 Gainesville, Florida, 32610, U.S., misaacson01@gmail.com

[b]Department of Chemistry, University of Florida, P.O. Box 117200 Gainesville, Florida, 32610, U.S., horen@chem.ufl.edu

[c]Department of Pharmacology and Therapeutics, University of Florida College of Medicine, P.O. Box 100267 Gainesville, Florida, 32610, U.S., clear@ufl.edu

[d]Department of Pharmacology and Therapeutics, University of Florida College of Medicine, P.O. Box 100267 Gainesville, Florida, 32610, U.S., wrkem@ufl.edu

[e]Department of Pharmacology and Therapeutics, University of Florida College of Medicine, P.O. Box 100267 Gainesville, Florida, 32610, U.S., rlpapke@ufl.edu

Abstract

The homomeric α7 nicotinic acetylcholine receptor is a well-studied therapeutic target, though its characteristically rapid desensitization complicates the development of drugs with specific agonist effects. Moreover, some experimental compounds such as GTS-21 (2,4diMeOBA), a derivative of the α7-selective partial agonist benzylidene anabaseine (BA), produce a prolonged residual desensitization (RD) in which the receptor remains non-activatable long after the drug has been removed from extracellular solution. In contrast, the desensitization caused by GTS-21's dihydroxy metabolite (2,4diOHBA) is relatively short-lived. RD is hypothetically due to stable binding of the ligand to the receptor in its desensitized state. We can attribute the reduction in RD to a single BA hydroxyl group on the 4' benzylidene position. Computational prediction derived

[1]This work was supported by National Institute of Health grant RO1-GM57481.

Corresponding author: Roger L. Papke, Phone: 352-392-4712, Fax: 352-392-9696, rlpapke@ufl.edu, Postal Address: Department of Pharmacology and Therapeutics, University of Florida College of Medicine, P.O. Box 100267 Gainesville, Florida, 32610, U.S., rlpapke@ufl.edu.
[2]Present address: 49 Convent dr. bldg. 49 rm. 1a16, Bethesda, MD, 20814, U.S.

Authorship Contributions
Participated in research design: Isaacson, Horenstein, and Papke
Conducted experiments: Isaacson and Stokes
Provided experimental tools (benzylidene anabaseines): Kem
Performed data analysis: Isaacson and Papke
Wrote or contributed to the writing of the manuscript: Isaacson, Horenstein, and Papke
Read and Commented on manuscript: Kem

from homology modeling showed the serine36 (S36) residue of α7 as a reasonable candidate for point-to-point interaction between BA compounds and the receptor. Through evaluating the activity of BA and simple derivatives on wild-type and mutant α7 receptors, it was observed that the drug-receptor pairs which were capable of hydrogen bonding at residue 36 exhibited significantly less stable desensitization. Further experiments involving the type II positive allosteric modulator (PAM) PNU-120596 showed that the various BA compounds' preference to induce either a PAM-sensitive (D_s) or PAM-insensitive (D_i) desensitized state is concentration dependent and suggested that both states are destabilized by S36 H-bonding. These results indicate that the fine-tuning of agonists for specific interaction with S36 can facilitate the development of therapeutics with targeted effects on ion channel desensitization properties and conformational state stability.

Keywords

conformational states; receptor desensitization; site-directed mutation; homology modeling

1. Introduction

Nicotinic acetylcholine receptors (nAChR) are transmembrane cation-selective ligand-gated ion channels, belonging to the large cysteine-loop superfamily of receptors, which include GABA, glycine, and serotonin-gated channels [1]. All nAChRs are pentameric in structure, comprised of protein subunits which form a ring around a central, water-filled pore. Seventeen unique subunits (α1–10, β1–4, γ, δ, and ε) have been identified, and most nAChRs are heteromeric, comprising both α and non-α subunits [2]. However, one of the most prevalent subtypes of neuronal nAChRs is homomeric, composed of five putatively identical α7 subunits. In the brain, such α7 receptors are found most abundantly in the hippocampus, thalamus, hypothalamus, and neocortex [3, 4]. The α7 receptor is distinguished by high calcium permeability, low probability of opening, and rapid desensitization following ligand binding. The α7 receptor has been implicated as influential in neuroprotection [5, 6, 7, 8], attentional and cognitive enhancement [9], and the regulation of inflammatory signaling [10, 11, 12], demonstrating its widespread influence and significance as a therapeutic target.

The α7 nAChR contains five potential ligand-binding domains (LBD) at the subunit interfaces, and at least a few structurally distinct allosteric sites [13]. In the absence of agonist, the channel exists in a resting "closed" state, preventing the flow of ions through its pore. Binding of agonist can temporarily promote conversion of receptors to a very short-lived, cation-permeable "open" conformational state or, more likely, to ligand-bound, closed states. These "desensitized" states are relatively stable as long as agonist is bound, preventing the receptor from any further activation. Upon complete drug washout from a population of desensitized receptors, some agonists such as acetylcholine will rapidly dissociate from the receptors, allowing them to return to the resting activatable state. Other agonists, such as nicotine or GTS-21, are capable of producing a form of desensitization from which the receptor takes significantly longer to recover [14]. This form of desensitization was first termed "residual inhibition or desensitization", since it was unclear whether the unresponsive state was due to the induction of ligand-bound nonconducting (desensitized) conformations or due to channel block. It was subsequently shown that although GTS-21 and nicotine could block the channel, such channel block was readily reversible, while the desensitization induced by these ligands was relatively stable [14]; therefore, we more accurately refer to the phenomenon simply as residual desensitization (RD).

Two distinct classes of desensitized conformational states have been identified for α7, referred to as the D_s and D_i states, distinguished by being sensitive or insensitive to conversion to open states by a type II [15] positive allosteric modulator (PAM), respectively [16]. RD may be associated with both D_s and D_i states, depending on the relative stabilities of these states, as determined by the chemical structure of the agonist and its interaction with the receptor binding pocket [17], as well as by the levels of PAM and agonist binding site occupancy [16]. The preferential induction of either D_s or D_i states may be an important consideration in the development of nAChR therapeutics, since the relative induction of these states would have significantly different effects when therapeutically combined with a type II PAM, and they also may be involved differently in intracellular signaling [16].

Benzylidene anabaseines (BAs) are one of several classes of α7-selective agonists [18], many of whose derivatives have been studied and observed to vary widely in potency and efficacy for activation [19]. Some BAs have therapeutic potential, such as 3-(2,4-dimethoxybenzylidene)anabaseine (alternatively called GTS-21, DMXBA, or 2,4diMeOBA), which has been shown to be an effective anti-inflammatory agent [11, 20] and has been proposed as a potential treatment for Alzheimer's disease [21] and schizophrenia [22]. This particular compound was shown to cause significant amounts of RD, while a dihydroxy analog (a GTS-21 metabolite *in vivo*), 3-(2,4-dihydroxybenzylidene)-anabaseine (2,4diOHBA), produces practically none [14]. Such significant differences in RD production resulting from minor differences in the agonist molecule may give clues as to the fundamental mechanism of desensitization. The purpose of this project was to investigate the mechanism of RD production or elimination, so that its modulation may be harnessed for the design of novel therapeutic compounds.

2. Materials and Methods

2.1 Reagents and Synthetic Chemistry

Solvents and reagents were purchased from Sigma-Aldrich Chemical Company (St. Louis, MO), Fisher scientific (Pittsburgh, PA) and TCI America (Portland, OR). PNU-120596 was synthesized following the method previously described [16, 23]. Benzylidene anabaseine compounds were synthesized by the reaction of anabaseine dihydrochloride with the appropriate benzaldehyde, as previously reported [24]. The purity of each BA dihydrochloride salt was verified by silica gel HPLC, NMR, mass spectral, and elemental analyses. NMR analysis indicated that the vinyl group in each compound was in the [E]configuration, as was found for other BAs [25]. The basicity, polarity, and rat nAChR binding properties of these compounds have been reported [26].

2.2 Molecular Modeling

A human α7 analog was created using the *Aplysia californica* AChBP structure (PDB ID 2WN9) as the template. The α7 sequence was modeled with SwissModel (http://swissmodel.expasy.org/). The resulting monomeric model was superimposed five times on each chain of the AChBP pentameric crystal structure in order to generate a pentameric model. The model was then examined for clashes, which were subsequently resolved by variation of side chain rotomers or in combination with an initial constrained minimization using the GROMOS force field resident in the SwissPDB viewer 4.0, followed by Amber 10 [27] molecular mechanics refinement with the bound 2WN9 ligand included. The model quality was assessed with the Molprobity server [28]. Docking was performed with Dock 6.5 [29].

2.3 cDNA Clones and RNA

The human α7 nAChR receptor clone was obtained from Dr. Jon Lindstrom (University of Pennsylvania, Philadelphia, PA), and the RIC-3 clone from Dr. Millet Treinin (Hebrew University, Jerusalem, Israel) for the purpose of co-injection with α7 to improve the level and speed of receptor expression [30]. Mutations at position 36 were introduced using the QuikChange Site-Directed Mutagenesis Kit (Agilent Technologies, Santa Clara, CA) following the manufacturer's instructions. Mutations were confirmed with automated fluorescent sequencing. After linearization and purification of cloned cDNA's, RNA transcripts were prepared using the appropriate mMessage mMachine kit from Ambion (Austin, TX).

2.4 Expression in *X. laevis* Oocytes

Oocytes were obtained from mature (>9cm) female *Xenopus laevis* African frogs (Nasco, Ft. Atkinson, WI). Frogs were anesthetized in 0.7 g/L solution of ethyl 3-aminobenzoate methanesulfonate buffered with sodium bicarbonate, followed by surgical removal of oocytes through an abdominal incision. Harvested oocytes were treated with 1.25 mg/ml collagenase (Worthington Biochemicals, Freehold, NJ) in calcium-free Barth's solution (88 mM NaCl, 1 mM KCl, 2.38 mM $NaHCO_3$, 0.82 mM $MgSO_4$, 15 mM HEPES, 12 mg/L tetracycline, pH 7.6) for 3–4 hours to remove the follicular layer. Stage-5 oocytes were isolated and injected with 50 nl (5–20 ng) of wild type (WT) or mutant α7 and RIC-3 cRNA. Suitable levels of receptor expression were typically achieved 2–6 days after injection of cRNA. For experiments involving the PAM PNU-120596, where standard levels of expression result in ion currents too large to be recorded in voltage clamp, experiments were typically conducted 1–3 days after RNA injection.

2.5 Electrophysiology

Two-electrode voltage clamp experiments were conducted using OpusXpress6000A (Molecular Devices, Sunnyvale, CA), an integrated system that provides automated impalement and voltage clamp of up to eight oocytes in parallel. Both the current and voltage electrodes were filled with 3 M KCl and oocytes were clamped at a holding potential of −60 mV. Data were collected at 50 Hz and filtered at 20 Hz. The oocytes were bath-perfused with Ringer's solution (115 mM NaCl, 10 mM HEPES, 2.5 mM KCl, 1.8 mM $CaCl_2$, pH 7.3), and agonist solutions were delivered from a 96-well drug plate using disposable tips. Flow rates were set at 2 ml/min, with each drug or control application delivered in 12 s durations followed by 181 s washouts with Ringer's unless noted otherwise.

2.6 Experimental Protocols and Data Analysis

Responses of α7 receptors and mutants to agonists were measured as both peak current and net charge measured over a 120 s period after solution application [31]. In most experiments, only net charge data are presented since the fast desensitization characteristic of α7 results in the peak current being reached before agonist solution exchange is complete, giving values which do not correspond to activation produced by the ligand at the final concentration applied. In experiments involving PNU-120596, however, the PAM eliminates the fast desensitization of α7 and allows peak currents to be used as a valid measurement of the receptor-mediated responses [16, 17].

Oocytes received two control ACh applications prior to receiving any drug in order to establish a steady reference response, and they received one or more control ACh applications at the end of all experiments. During concentration-response curve (CRC) experiments, alternating applications of experimental drug and ACh control were delivered

to determine whether cells retained their initial responsiveness to ACh throughout the experiment. If responses to ACh controls remained constant (varying <25% from the previous control), responses to drugs were normalized to the response of the preceding control for each cell individually. For experiments where control responses were not stable, typically observed at higher drug concentrations where RD was produced, those concentrations of drugs were delivered to cells in separate experiments and normalized similarly. RD curves were generated in parallel to the CRC experiments by measuring the reduced control response after each drug application relative to the control preceding it. For experiments involving drug incubation through bath applications, all responses were normalized to the average of two ACh control responses taken immediately prior to the switch of bath solution, for each cell individually. These normalization procedures had the effect of compensating for differing levels of receptor expression among the multiple oocytes used in each experiment. Each experiment was conducted on at least four oocytes, with mean values and standard errors (S.E.M.) calculated from their normalized responses.

For concentration-response relations, data were plotted using Kaleidagraph 3.0.2 (Abelbeck/Synergy, Reading, PA). Curves were generated using the Hill equation:

$$\text{Response} = I_{max}[\text{agonist}]^n/([\text{agonist}]^n + (EC50)^n)$$

where I_{max} denotes the maximal response for a particular agonist/subunit pair, and n represents the Hill coefficient. I_{max}, n, EC_{50}, and IC_{50} were all unconstrained for the fitting procedures. For inhibition (RD) curves, the initial I_{max} was constrained to 1 and the Hill slope fit to a negative value.

3. Results

3.1 Benzylidene Anabaseine CRCs on α7 nAChR

We previously reported [14] a significant difference in RD from GTS-21 (2,4diMeOBA) and its dihydroxy analog, (E)-3-(2, 4-dihydroxybenzylidene)-anabaseine (2,4DiOHBA). The multiple hydroxyl groups of 2,4DiOHBA obfuscated our ability to determine precisely what molecular interactions may be occurring between the drug and receptor at a single points, so the first goal of this project was to attempt to determine if a reduction of RD could be attributed to a single hydroxyl group on BA. Since 2MeO4OHBA (4OH-GTS-21) was also known to produce relatively little RD, the 4' position of BA was chosen for investigation, creating 3-(4-hydroxybenzylidene)anabaseine (4OHBA). For comparison, the analogous methylated version of BA (4MeBA) was also investigated. These compounds are shown in Figure 1A. CRCs were obtained for BA, 4OHBA, and 4MeBA on the α7 receptor (example Figure 1B) and were normalized to the maximal response of α7 to ACh, shown in Figure 1C. RD was sometimes evident as a decrease in the ACh-evoked responses following the application of the BA compounds (see section 2.6). The concentration dependence for this effect was also calculated for these three BA compounds, shown in Figure 1D. Note that when RD occurred, the progressive testing of single cells, as illustrated in Figure 1B, was discontinued, and additional experiments were conducted with single high concentrations of the BA compounds on new sets of cells (see section 2.6).

The results in Figures 1C and 1D show that at the concentration where 4MeBA produced its greatest evoked response (approximately 300 μM), post-controls (responses to control ACh applications which follow after the test drug applications) were reduced by 80%, indicative of strong RD. 4OHBA, despite having significantly greater potency than BA and 4MeBA, only reduced post-control responses 10–20% at concentrations required to promote maximal evoked responses (30 μM – 300 μM).

3.2 Ligand binding-site modeling

With the significantly lower levels of RD associated with the presence of a group capable of hydrogen bonding at the BA 4' position, computational prediction derived from homology modeling was performed to determine which residues in the α7 LBD (shown in Figure 2A) may be interacting with the hydroxyl group. AChBP crystallized with the benzylidene motif agonist, 4OH-GTS-21 (2MeO4OHBA), was used as the template to generate the homology model. As shown in Figure 2B, the serine residue at position 36 (S36) was the most likely candidate for interaction through hydrogen bonding with 4OHBA. From this observation, we hypothesized that the potential for an agonist molecule to form an H-bond to the residue at position 36 would be inversely related to the amount of RD it can produce.

3.3 BA compounds on S36 mutant receptors

Five amino acids with hydrophobic side groups of various sizes were chosen for α7 point mutations in this study, to test whether a low level of RD is due to hydrogen bonding between the agonist molecule and residue S36, specifically. Both small and large hydrophobic groups were chosen to correct for possible differences in steric relationships between serine and any other chosen residue. The five chosen mutant residues were glycine (G), alanine (A), cysteine (C), valine (V), and isoleucine (I), whose differing side groups are displayed in Figure 3A.

Prior to analyzing the effects these various point mutations had on the receptors' responses to BA compounds, it was determined whether expression of these mutants produced receptors with function comparable to WT α7. Oocytes injected with the WT and various mutant receptor cRNA were treated with 3 mM ACh, and their absolute net charge responses were compared relative to the WT responses obtained on the same day post-injection with the same lot of oocytes. These results are summarized in Figure 3B, showing that all mutants were functional to varying degrees. For all subsequent experiments, each oocyte's test responses were normalized to its own control response to ACh in order to compensate for differing propensities for expression, inherent values of P_{open}, and responsiveness relative to ACh.

CRCs for ACh were generated for all mutant receptors (Figure 4A) to compare their responses to this small agonist, and to serve as a point of comparison for the BA compounds. The potencies estimated from these curves are shown in the first column of Table 1. ACh showed very similar potency with WT and all mutants other than for S36I receptors, indicating that the mutations, aside from the change of serine to isoleucine, likely did not cause major changes to the ACh activity profile. CRCs (Figure 4 B–F) and RD curves (not shown) were also obtained for all three BA compounds on all mutant receptors; summarized in Tables 1 and 2.

Three important observations can be made from these results. The first is that the S36I mutant, which, as noted in Figures 3 and 4A, was relatively non-responsive to ACh, was further compromised in responses to the BA compounds. BA and 4MeBA had the lowest efficacy and potency for this mutant as compared to the other S36 mutants. Responses to BA relative to ACh were also reduced compared to WT. It is likely that the S36I mutation produced a general loss of function. A second observation is that, similar to what was observed with the WT α7 receptor in Fig 1C, 4OHBA had greater efficacy and potency for activation on all S36 mutants as compared to BA and 4MeBA, with particularly large increases in potency and efficacy for the G and A mutants. This might suggest that the basic activation properties of 4OHBA on the α7 receptor do not require any specific interaction with Ser36, and may even be slightly hindered by it. A third important general observation is that the RD manifested with the WT receptor with 4OHBA was lower than any other

combination, leading to a calculated IC_{50} far greater than the concentration range studied. Since WT-4OHBA was the only drug-receptor pair which can H-bond at the S36 position, it is reasonable to hypothesize that it is this interaction specifically that minimized RD. Additionally, the RD produced by the hydrophobic compounds was increased for specific mutants.

3.4 Properties of desensitized states

The potential hydrogen bonding between the 4OH group of 4OHBA and S36 appears to not support the stability of a conformational state(s) associated with RD; RD was observed even with 4OHBA when S36 was mutated to a hydrophobic residue. Experiments were then conducted to determine the properties of the conformational state(s) favored for each drug-receptor pair in regard to PAM-sensitive (D_s) and PAM-insensitive (D_i) desensitized states.

After a 5-minute bath application of each BA compound, assumed to be an adequate amount of time for the receptor to equilibrate into its most favorable conformational state in the presence of the agonist, a bolus of 1mM ACh (a concentration which can elicit a maximal agonist response) was applied to each receptor to determine whether and to what degree the receptor in this conformational state was still capable of activation (i.e. as a measure of total desensitization). After washout of the drug bath, two control ACh applications were delivered to observe if any RD was still present. In addition to the BA compounds, a 5-minute bath application of Ringer's was performed as a zero desensitization control, assumed to leave the receptors in the state maximally responsive to ACh and with minimal induction of RD (only what would be caused by the 1mM ACh application). Data were also compared to a 5-minute 300 μM ACh bath application, predicted to leave the receptors completely unresponsive to additional ACh and also producing minimal RD [14]. The experimental protocol and results of these experiments are shown in Figure 5. The S36I mutant was omitted from these experiments due to its general deficiency in function and atypical responses to ACh, as previously observed.

As expected, the cells that received the 5-minute incubation in Ringer's were fully responsive to the ACh probe, showed minimal desensitization in the first post-control (indicative of low RD), and were fully recovered by the second post-control. Likewise, although the cells exposed to the 5-minute ACh bath application were fully desensitized to the further application of ACh, they all recovered to pre-incubation control levels by the second post-incubation ACh control application. For cells incubated with the BA compounds (Figure 5C), the RD observed in the post-controls were generally consistent with IC_{50} values in Table 2 for each drug-receptor pair, with 4MeBA generally producing large amounts of RD and BA producing relatively less RD than 4MeBA. However, following incubations with 4OHBA, only the WT receptor fully recovered during the post-controls, further showing that the potential H-bonding combination in wild type specifically reduced the stability of the desensitized states.

Seemingly unaffected by the identity of residue 36, all receptors were most excitable by ACh immediately following incubation with BA and least with 4OHBA. This trend appeared to correlate to each drug's potency for agonism (higher potency resulting in lower ACh excitability), consistent with the more potent 4OHBA producing more desensitization after a 5-minute incubation than the less potent BA.

Additionally, a most remarkable exception to 4OHBA’s tendency to produce low RD on the WT receptor was observed with S36G using this protocol. Subsequent ACh control responses were very strongly inhibited after the 5-minute incubation and the application of the 1 mM ACh probe. With our standard protocol for measuring RD (using 12 s applications, as illustrated in Figure 1), we estimated the IC_{50} for 4OHBA on S36G to be

130 ± 20 μM (Table 2), yet following a 5-minute incubation in a concentration well under that IC_{50} value, there was a nearly complete suppression of the ACh control responses. To confirm that this was an effect of the prolonged incubation with 4OHBA, we conducted a similar set of experiments, omitting the 1 mM ACh probe application and using various durations of 4OHBA incubations. The results (Figure 6) suggest that this form of RD was dependent on incubation time as well as incubation concentration.

A protocol similar to the one used for the experiments illustrated in Figure 5 was used to determine the degree to which the desensitization detected by reduced responses to 1 mM ACh represented the induction of D_s vs. D_i states. Specifically, in these experiments a bath application of 30 μM of the type II PAM, PNU-120596 (PNU, Figure 7) was applied after the drug bath instead of ACh (as in Figure 5), so that receptors in the D_s state would be visibly activated by the addition of PNU and those in the D_i state would not. As expected, the application of PNU-120596 produced no responses following the Ringer's control bath incubations (Figure 7A). As shown in Figure 5, ACh incubations were fully desensitizing for both the WT and all of the S36 mutants. However, the responses to PNU-120596 application following ACh incubations (Figure 7) show that the receptors varied in their relative responses to PNU-120596, indicative of differing levels of D_s induced by the same agonist. Specifically, compared to WT, the induction of D_s was significantly greater for S36V and less for S36C ($p < 0.05$). For BA, we saw that PNU-120596 effects (D_s induction) were significantly greater than the other BA compounds, and less for S36A and S36V compared to WT ($p < 0.05$, Figure 7C). In contrast, 4OHBA produced relatively little D_s for WT, and this was not increased in the mutants and actually reduced for S36C compared to WT ($p < 0.05$).

In these experiments, the post-controls were influenced by interacting factors including: the persistence of PNU-120596 potentiation, which can require several minutes of washout to be fully reversed [14]; the amount of RD present, which may convert between D_s to D_i as functions of time, ligand, and residue [17]; and also the reversal of the RD itself, which may or may not have been affected by the PNU-120596 treatments. Due to these complications we would refrain from making any interpretations of the post-control responses in Figure 7, although it is interesting to note generally low responses of the mutants incubated in 4OHBA as compared to the WT, even after the application of PNU-120596.

Since both the levels of ACh excitability in Figure 5 and PNU modulation in Figure 7 generally tracked to each drug's potency to each receptor (greater potency producing less excitability and less D_s state modulation), we hypothesized that the propensity for each BA compound to promote either the D_s or D_i state depended on the level of binding site occupancy rather than just on the identity of the binding ligand (low-intermediate occupancy favors D_s state, high occupancy favors D_i state), a phenomenon that has been recently reported for ACh on α7 [16]. Since BA and 4MeBA each have lower potency for activation of WT α7 than does 4OHBA, we conducted additional experiments with the ligands at additional concentrations to determine if there were parallel shifts in desensitization and the induction of D_s. These bath experiments were repeated using only the WT receptor, though this time using concentrations of each drug both above and below their respective EC_{50}s for WT α7, (as describe in the Figure legend). The higher drug concentrations were chosen to produce complete binding-site occupancy and lower concentrations to produce equivalent amounts of intermediate occupancy (as predicted from its partial ACh excitability relative to the Ringer's controls in Figure 5A). The results of these experiments are shown in Figure 8A–C.

Our expectation was that for all of the BA compounds, responses to an ACh probe would be decreased at the higher test concentration (representing high binding-site occupancy) and, as

shown in Figure 8A, this was confirmed. Also, as expected, for the RD-producing hydrophobic BAs the post-controls were more effectively decreased at the higher concentrations (Figure 8B), while there was no significant difference in the controls following incubations in low or high concentrations of 4OHBA (as it produces little RD on the WT receptor at any concentration). Our predictions for the PNU-evoked responses were less clear, since the desensitization measured relative to the ACh probes might have represented either D_s or D_i; however, as expected, the largest currents evoked by PNU-120596 were observed for the partially desensitizing low concentrations of the RD-producing BA and 4MeBA (Figure 8C). Following incubations with higher concentrations of these compounds, receptors appeared to be induced exclusively into D_i. In contrast, with the 4OHBA compound, fewer receptors resided in the D_s state following a low-concentration incubation, and receptors did not significantly favor the D_i state following the high-concentration incubation.

3.5 BA compounds on an S36T mutant receptor

The results obtained with the initial series of mutants suggested the hypothesis that H-bonding between a BA compound with a hydroxyl at the 4 position and the S36 residue of α7 produces had the specific effect of destabilizing desensitization which was measurable as a decrease or elimination of RD. In order to test this hypothesis we created an S36T mutant. Although threonine is sterically different from serine, it could retain an ability to H-bond to 4OHBA, and if our assumption is correct, should also experience significantly less RD from 4OHBA than from BA or 4MeBA. Expression tests (not shown) indicated that the S36T functioned at least as well as WT α7. CRC's (Figure 9A) and RD curves (Figure 9B) similar to those in Figure 1 were obtained for ACh and the 3 BA compounds on S36T (Table 1), and while all 3 BA compounds produced less RD on S36T than they did on the WT receptor, 4OHBA caused significantly less than the other 2, as expected (Table 2).

4. Discussion

While tetramethylammonium, the minimal structure able to act as a full agonist for neuronal nAChR, is small enough to bind entirely within the hydrophobic pocket encompassed by the alpha subunit C-loop, larger agonists, such as the α7-selective compounds utilizing the benzylidene motif [18], appear to bind in space that extends into the intersubunit interface [32]. We have previously shown that the chemical character of specific compounds in this extended domain importantly regulates functional properties such as potency, efficacy, and the induction of stable desensitization [14]. Most notably, compounds with one or more hydroxyl groups on the benzene ring have improved efficacy for human α7 receptors compared to compounds lacking these substitutions or with more hydrophobic substitutions [24]. Our present work suggests that for compounds with substitutions at the 4 position, the effects of hydroxyl groups rely on specific interactions with the S36 residue on the complementary surface of the LBD. Specifically, H-bonds between the 4 position of the benzylidene group and S36 may favor the stability of an activatible state over that of the relatively stable form of desensitization associated with RD, and ultimately with the induction of D_i (Figure 8).

While the S36 residue is of key importance for the activating properties of BA compounds, replacement of serine with small amino acids had little impact on activation by ACh. This supports the hypothesis that the activation by the "core" agonist is relatively independent of this site and that this residue is a candidate for interactions with the extended BA "selectophore". In contrast, the replacement of S36 with cysteine, valine, or isoleucine appeared to have more global effects on receptor function or expression, so that we should be relatively circumspect in regard to the effects of these mutations on the activity of the BA

compounds. This is particularly the case for the S36I mutant, which showed a large decrease in ACh potency and was therefore excluded from some of the later experiments.

The G and A mutations had relatively little effect on the profile of BA, although RD was increased with 36A compared to 36G, making it interesting to speculate that the difference in size between these residues was enough to change the interactions with the unsubstituted ring. Conversion of the S36 to G or A produced a large increases in efficacy of 4OHBA relative to ACh and parallel shifts in potency for both activation and for RD. For 4MeBA both the G and A mutations increased potency for activation, but only G increased efficacy and caused a parallel increase in the potency of 4MeBA for RD.

Surprisingly large amounts of current were evoked by the 1 mM applications of ACh following prolonged exposure to BA for WT and all the mutants other than 36C, and for 36G the responses to ACh remained large after 4MeBA. The concentration of BA for these experiments (Figure 4) was at about the EC_{50}, yet cells were still responsive to additional ACh. This indicates that, even in the prolonged presence of agonist at the EC_{50} concentration, not all of the α7 receptors become desensitized; that is, receptors do not progressively enter deep desensitized states over the course of these incubations. This is consistent with the hypothesis that concentrations which are most efficacious for activation do not saturate the binding sites and that, unlike heteromeric nAChR, α7 receptors do not greatly increase in their affinity for binding agonist following channel activation (i.e. concomitant to desensitization).

The PNU effects were greater on the BA-soaked cells (Figure 7) than the ACh-soaked cells, even though the apparent desensitization was greater with the ACh soaks (Figure 5). Hypothetically, this was due to the fact that the ACh concentration was 10-fold higher than the EC_{50} and induced mostly D_i. The relationship between partial desensitization by BA and 4MeBA and best induction of D_s is also borne out in Figure 8. Consistent with our previous studies with ACh and WT [16], high occupancy by these compounds efficiently promotes D_i preferentially. Why is the 4OHBA different? Our data suggest that it is because D_i is intrinsically less stable with the OH-serine interaction.

The observation that large amounts of RD were induced in the S36G mutant by prolonged incubation with 4OHBA suggests that the induction of some conformational states by specific ligands is time dependent and that reversibility (time constant of recovery) is also a factor that needs to be considered. Our data suggest that the potential hydrogen bonding of a benzylidene anabaseine derivative to S36 is associated with a low level of RD and that disruption of this potential interaction can lead to an increase in potency for activation and desensitization and increased efficacy. When the potential H-bond interaction for the 4OHBA-WT α7 pair is eliminated, the production of RD is increased and, at least in the case of S36G, increases progressively with prolonged incubation. It is interesting to speculate what might be the cause for this time dependency.

Insights into the significance of point-to-point ligand-receptor interactions at S36 may come from structural analysis of α7 which was deduced from x-ray crystallography on AChBP after incubation in 400–500μM of GTS-21 and 4OH-GTS-21 (concentrations that our data would suggest cause complete receptor occupancy) [32]. GTS-21 was observed to occupy all 5 binding sites, conforming in orientation 1 (similar to the docking shown in Figure 2A) in 2 sites and equally distributed between orientation 1 and an alternative orientation 2 in the other 3 sites (Figure 10A). Conversely, 4OH-GTS-21 conformed to a state very similar to state 1 in all 5 binding sites. State 1 places the 4OH and the S36 residue close together, while state 2 significantly separates them. Note that Figure 10A presents the AChBP model, having threonine at position 36 rather than serine. If agonists residing in state 2 more highly

promote stable desensitized states, and D_i in particular (Figure 10B), then S36 H-bonding might explain why 4OHBA discourages the desensitized states by favoring the state 1 orientation. It is possible that disruption of the potential H-bond between 4OHBA and S36 might lower the relative stability of orientation 1 and that in hydrophobic S36 mutants over time the 4OHBA binding might accumulate in orientation 2, which could be more associated with RD.

Unfortunately, the crystal structure analyses shed light on only the fully occupied α7 receptor, which we show to be more associated with the D_i state. For the experiments shown in Figure 8, the assumption of intermediate binding-site occupancy had to be based on intermediate ACh excitability, which could have resulted either from ACh's ability to excite a receptor with partial BA occupancy or from the existence of a fraction of receptors with no bound ligand at all. If only a fraction of receptors were to be occupied with any amount of ligand, and since no positive (or negative) binding cooperativity is currently known to exist for the α7 receptor, it is most reasonable to predict that only a fraction of the receptor binding sites will be occupied on any given receptor. However, it may still be very useful if similar crystallography experiments could be performed using ligand concentrations shown in this project to produce partial binding-site occupancy.

We have introduced RD as a general term to describe desensitization which is not quickly reversed after agonist washout, and both D_s and D_i states can be associated with RD, though not in equivalent ways. At intermediate occupancy of the agonist binding sites, in which the D_s state is favored by BA and 4MeBA (Figure 8), the 3 minutes inbetween the first and second post-controls is enough time to see significant, though not complete, receptor resensitization (data not shown). However, at full occupancy and complete D_i state preference by BA and 4MeBA, practically no recovery is made between the 2 post-controls, suggesting that, as previously understood, the D_i state is generally more stable and therefore more likely associated with longer-lasting RD than the D_s state [16]. This may partly explain the rapid reversibility of desensitization caused by ACh, as receptors are never completely removed from the D_s state (Figure 7B).

In summary, we confirm that making simple changes to the core BA agonist significantly alters its effects on the α7 receptor, and we have identified a key point-to-point interaction responsible for some of these differences. One therapeutic implication of the findings in this study is that compounds such as BA and 4MeBA may produce very different effects at different concentrations. Over a ten-fold concentration range of BA or 4MeBA, available receptors change from residing in an intermediately stable D_s state to a more stable D_i state (Figure 8C). In contrast, 4OHBA, and most likely 4OH-GTS-21 as well, caused similar RD and D_s state preference at both high and low concentrations (Figure 8B–C). While much care must be taken in predicting effective doses of therapeutic BA compounds which cannot H-bond to S36 in order to balance effects of agonism and desensitization, compounds such as 4OHBA may just require consideration of effective levels of agonism only. In addition, combination therapies involving compounds similar to 4OHBA along with a type II PAM may never produce the cytotoxic levels of channel opening that has been observed with ACh or choline [33], as 4OHBA may only ever allow relatively modest potentiation by the PAM.

Acknowledgments

Some of the syntheses of the benzylidene anabaseines were conducted by Dr. F. Soti (University of Florida, Department of Pharmacology and Therapeutics). We thank Shehd A. A. Al Rubaiy, Sara Copeland, Matthew R. Kimbrell, Lu Wenchi Corrie, and Thomas F. Pack for conducting the OpusXpress experiments and Natalia Diaz-Torres for assistance in some of the oocyte experiments and in the production of S36 mutants. We also thank Dr. Lynn Wecker (University of South Florida) for the use of an additional OpusXpress 6000. This work was supported by National Institute of Health grant RO1-GM57481.

Abbreviations

ACh	acetylcholine
nAChR	nicotinic acetylcholine receptor
BA	benzylidene anabaseine
RD	residual desensitization
PAM	positive allosteric modulator
LBD	ligand-binding domain
CRC	concentration-response curve

Structure-based names

2,4diMeOBA (GTS-21)	3-(2,4-dimethoxybenzylidene)anabaseine
2,4diOHBA	3-(2,4-dihydroxybenzylidene)anabaseine
PNU-120596	*N*-(5-Chloro-2,4-dimethoxyphenyl)-*N*′-(5-methyl-3-isoxazolyl)-urea
4OHBA	(E)-3-(4-hydroxybenzylidene)anabaseine
4MeBA	3-(4-methylbenzylidene)anabaseine

References

1. Millar NS, Gotti C. Diversity of vertebrate nicotinic acetylcholine receptors. Neuropharmacology. 2009; 56(1):237–246. [PubMed: 18723036]
2. Dani JA, Bertrand D. Nicotinic acetylcholine receptors and nicotinic cholinergic mechanisms of the central nervous system. Ann Rev Pharmacol Toxicol. 2007; 47:699–729. [PubMed: 17009926]
3. Paterson D, Nordberg A. Neuronal nicotinic receptors in the human brain. Prog Neurobiol. 2000; 61(1):75–111. [PubMed: 10759066]
4. Seguela P, Wadiche J, Dinely-Miller K, Dani JA, Patrick JW. Molecular cloning, functional properties and distribution of rat brain alpha 7: a nicotinic cation channel highly permeable to calcium. J Neurosci. 1993; 13(2):596–604. [PubMed: 7678857]
5. Dajas-Bailador FA, Lima PA, Wonnacott S. The alpha7 nicotinic acetylcholine receptor subtype mediates nicotine protection against NMDA excitotoxicity in primary hippocampal cultures through a Ca(2+) dependent mechanism. Neuropharmacology. 2000; 39(13):2799–2807. [PubMed: 11044750]
6. Marrero MB, Bencherif M. Convergence of alpha 7 nicotinic acetylcholine receptor-activated pathways for anti-apoptosis and anti-inflammation: central role for JAK2 activation of STAT3 and NF-kappaB. Brain Res. 2009; 1256:1–7. [PubMed: 19063868]
7. Ren K, Puig V, Papke RL, Itoh Y, Hughes JA, Meyer EM. Multiple calcium channels and kinases mediate alpha7 nicotinic receptor neuroprotection in PC12 cells. J Neurochem. 2005; 94(4):926–933. [PubMed: 15969741]
8. Svensson AL, Nordberg A. Beta-estradiol attenuate amyloid beta-peptide toxicity via nicotinic receptors. Neuroreport. 1999; 10(17):3485–3489. [PubMed: 10619630]
9. Young JW, Finlayson K, Spratt C, Marston HM, Crawford N, Kelly JS, et al. Nicotine improves sustained attention in mice: evidence for involvement of the alpha7 nicotinic acetylcholine receptor. Neuropsychopharmacology. 2004; 29(5):891–900. [PubMed: 14970827]
10. Giebelen IA, van Westerloo DJ, LaRosa GJ, de Vos AF, van der Poll T. Local stimulation of alpha7 cholinergic receptors inhibits LPS-induced TNF-alpha release in the mouse lung. Shock. 2007; 28(6):700–703. [PubMed: 17621262]

11. Pavlov VA, Ochani M, Yang LH, Gallowitsch-Puerta M, Ochani K, Lin X, et al. Selective alpha7-nicotinic acetylcholine receptor agonist GTS-21 improves survival in murine endotoxemia and severe sepsis. Crit Care Med. 2007; 35(4):1139–1144. [PubMed: 17334244]
12. Wang H, Yu M, Ochani M, Amella CA, Tanovic M, Susarla S, et al. Nicotinic acetylcholine receptor alpha7 subunit is an essential regulator of inflammation. Nature. 2003; 421(6921):384–388. [PubMed: 12508119]
13. Bertrand D, Bertrand S, Cassar S, Gubbins E, Li J, Gopalakrishnan M. Positive allosteric modulation of the alpha7 nicotinic acetylcholine receptor: ligand interactions with distinct binding sites and evidence for a prominent role of the M2–M3 segment. Mol Pharmacol. 2008; 74(5): 1407–1416. [PubMed: 18678621]
14. Papke RL, Kem WR, Soti F, López-Hernández GY, Horenstein NA. Activation and desensitization of nicotinic alpha7-type acetylcholine receptors by benzylidene anabaseines and nicotine. J Pharmacol Exp Ther. 2009; 329(2):791–807. [PubMed: 19223664]
15. Gronlien JH, Hakerud M, Ween H, Thorin-Hagene K, Briggs CA, Gopalakrishnan M, et al. Distinct profiles of alpha7 nAChR positive allosteric modulation revealed by structurally diverse chemotypes. Mol Pharmacol. 2007; 72(3):715–724. [PubMed: 17565004]
16. Williams DK, Wang J, Papke RL. Investigation of the Molecular Mechanism of the Alpha7 nAChR Positive Allosteric Modulator PNU-120596 Provides Evidence for Two Distinct Desensitized States. Mol Pharmacol. 2011; 80(6):1013–1032. [PubMed: 21885620]
17. Wang J, Papke RL, Stokes C, Horenstein NA. Potential state-selective hydrogen bond formation can modulate the activation and desensitization of the alpha7 nicotinic acetylcholine receptor. J Biol Chem. 2012; 287(26):21957–21969. [PubMed: 22556416]
18. Horenstein NA, Leonik FM, Papke RL. Multiple pharmacophores for the selective activation of nicotinic alpha7-type acetylcholine receptors. Mol Pharmacol. 2008; 74(6):1496–1511. [PubMed: 18768388]
19. Papke RL, Meyer EM, Lavieri S, Bollampally S, Papke T, Horenstein B, et al. Effects at a distance in alpha7 nAChR selective agonists: Benzylidene substitutions regulate potency and efficacy. J Neuropharm. 2004; 46(7):1023–1038.
20. Kox M, van Velzen JF, Pompe JC, Hoedemaekers CW, van der Hoeven JG, Pickkers P. GTS-21 inhibits pro-inflammatory cytokine release independent of the Toll-like receptor stimulated via a transcriptional mechanism involving JAK2 activation. Biochem Pharmacol. 2009; 78(7):863–872. [PubMed: 19576181]
21. Kem WR. The brain alpha7 nicotinic receptor may be an important therapeutic target for the treatment of Alzheimer's disease: studies with DMXBA (GTS-21). Behav Brain Res. 2000; 113(1–2):169–181. [PubMed: 10942043]
22. Freedman R, Olincy A, Buchanan RW, Harris JG, Gold JM, Johnson L, et al. Initial phase 2 trial of a nicotinic agonist in schizophrenia. Am J Psychiatry. 2008; 165(8):1040–1047. [PubMed: 18381905]
23. Piotrowski DW, Rogers BN, McWhorter WW Jr, Walker DP, Corbett JW, Groppi VE Jr, et al. Preparation of ureas as positive allosteric modulators of the nicotinic acetylcholine receptor. Pharmacia & Upjohn Company, USA. 2003
24. Kem WR, Mahnir VM, Prokai L, Papke RL, Cao X, Le Francois S, et al. Hydroxy metabolites of the Alzheimer's drug candidate DMXBA (GTS-21): their molecular properties, interactions with brain nicotinic receptors and brain penetration. Mol Pharm. 2004; 65(1):56–67.
25. Zoltewicz JA, Prokai-Tatrai K, Bloom L. Long range transmission of polar effects in cholinergic 3-arylideneanabaseines. Conformations calculated by molecular modelling. Heterocycles. 1993; 35(1):171–179.
26. Slavov SH, Radzvilovits M, LeFrancois S, Stoyanova-Slavova IB, Soti F, Kem WR, et al. A computational study of the binding of 3-(arylidene) anabaseines to two major brain nicotinic acetylcholine receptors and to the acetylcholine binding protein. Eur J Med Chem. 2010; 45(6): 2433–2446. [PubMed: 20236734]
27. Case, DA.; Darden, TA.; Cheatham, TE.; Simmerling, CL.; Wang, J.; Duke, RE., et al. Amber 10. San Francisco: University of California; 2008.

28. Chen VB, Arendall WB 3rd, Headd JJ, Keedy DA, Immormino RM, Kapral GJ, et al. MolProbity: all-atom structure validation for macromolecular crystallography. Acta Crystallogr D Biol Crystallogr. 2010; 66(Pt 1):12–21. [PubMed: 20057044]

29. Moustakas DT, Lang PT, Pegg S, Pettersen E, Kuntz ID, Brooijmans N, et al. Development and validation of a modular, extensible docking program: DOCK 5. J Comput Aided Mol Des. 2006; 20(10–11):601–619. [PubMed: 17149653]

30. Halevi S, Yassin L, Eshel M, Sala F, Sala S, Criado M, et al. Conservation within the RIC-3 gene family. Effectors of mammalian nicotinic acetylcholine receptor expression. J Biol Chem. 2003; 278(36):34411–34417. [PubMed: 12821669]

31. Papke RL, Papke JKP. Comparative pharmacology of rat and human alpha7 nAChR conducted with net charge analysis. Br J of Pharm. 2002; 137(1):49–61.

32. Hibbs RE, Sulzenbacher G, Shi J, Talley TT, Conrod S, Kem WR, et al. Structural determinants for interaction of partial agonists with acetylcholine binding protein and neuronal alpha7 nicotinic acetylcholine receptor. EMBO J. 2009; 28(19):3040–3051. [PubMed: 19696737]

33. Williams DK, Peng C, Kimbrell MR, Papke RL. Intrinsically Low Open Probability of α7 Nicotinic Acetylcholine Receptors Can Be Overcome by Positive Allosteric Modulation and Serum Factors Leading to the Generation of Excitotoxic Currents at Physiological Temperatures. Mol Pharmacol. 2012; 82(4):746–759. [PubMed: 22828799]

34. Horenstein NA, McCormack TJ, Stokes C, Ren K, Papke RL. Reversal of agonist selectivity by mutations of conserved amino acids in the binding site of nicotinic acetylcholine receptors. J Biol Chem. 2007; 282(8):5899–5909. [PubMed: 17189260]

35. Williams DK, Stokes C, Horenstein NA, Papke RL. Differential regulation of receptor activation and agonist selectivity by highly conserved tryptophans in the nicotinic acetylcholine receptor binding site. J Pharmacol Exp Ther. 2009; 330(1):40–53. [PubMed: 19339660]

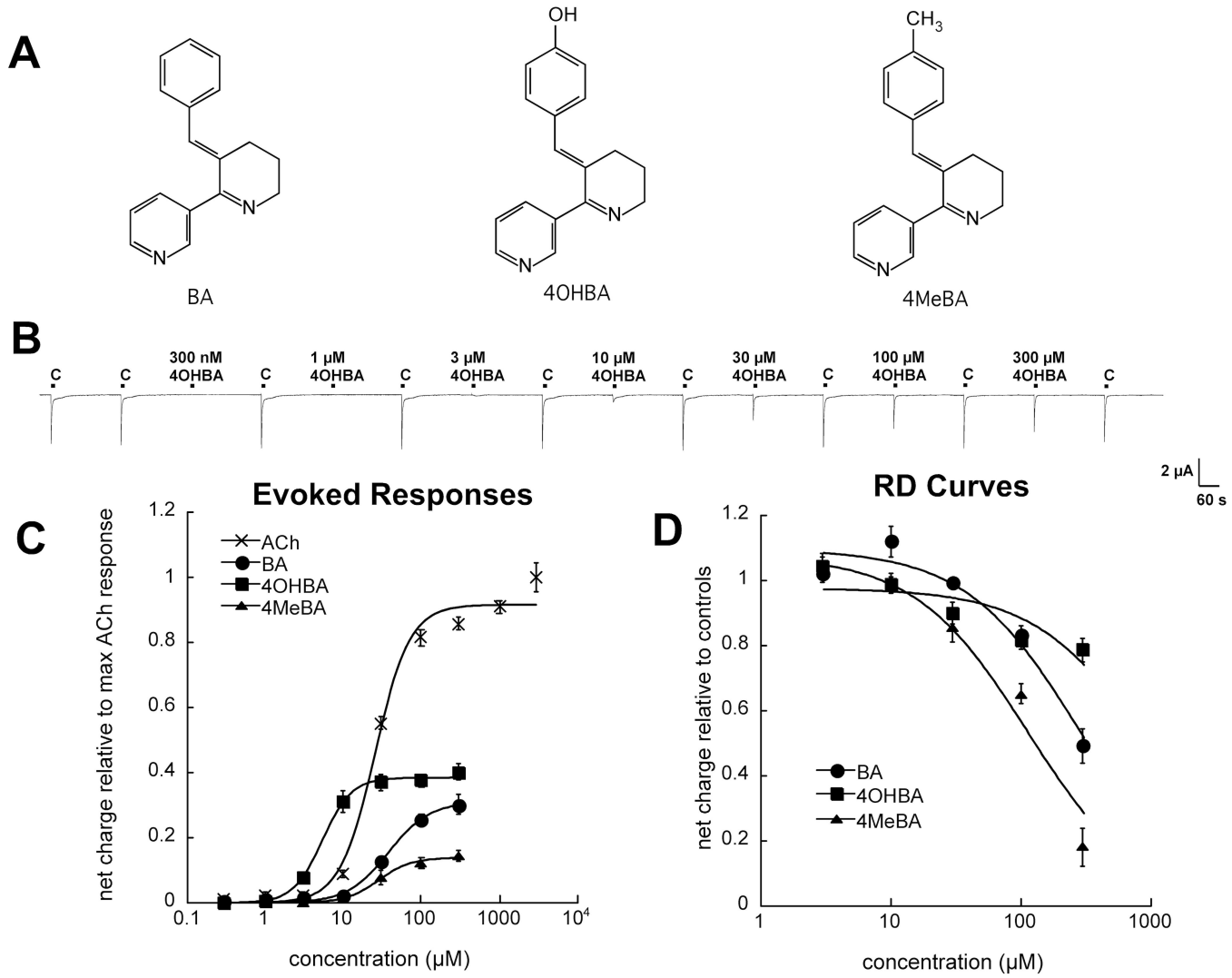

Figure 1. Benzylidene anabaseines and their effects on the α7 nAChR

A) Structures of benzylidene anabaseine (BA), and homologues (E)-3-(4-hydroxybenzylidene)anabaseine (4OHBA) and (E)-3-(4-methylbenzylidene)anabaseine (4MeBA). **B**) Sample raw data trace for the 4OHBA CRC on WT α7. **C**) CRCs for ACh, BA, 4OHBA, and 4MeBA on the WT α7 receptor. Points were generated by calculating the area of each test response relative to the response by the preceding ACh control and then normalized to the maximal ACh response, observed at 3mM ACh. **D**) RD curves for BA, 4OHBA, and 4MeBA on WT α7. Points were generated by calculating the area of each control response immediately following a test application relative to the control response preceding that application. For panels C & D all points are the averages (±SEM) of at least four oocytes.

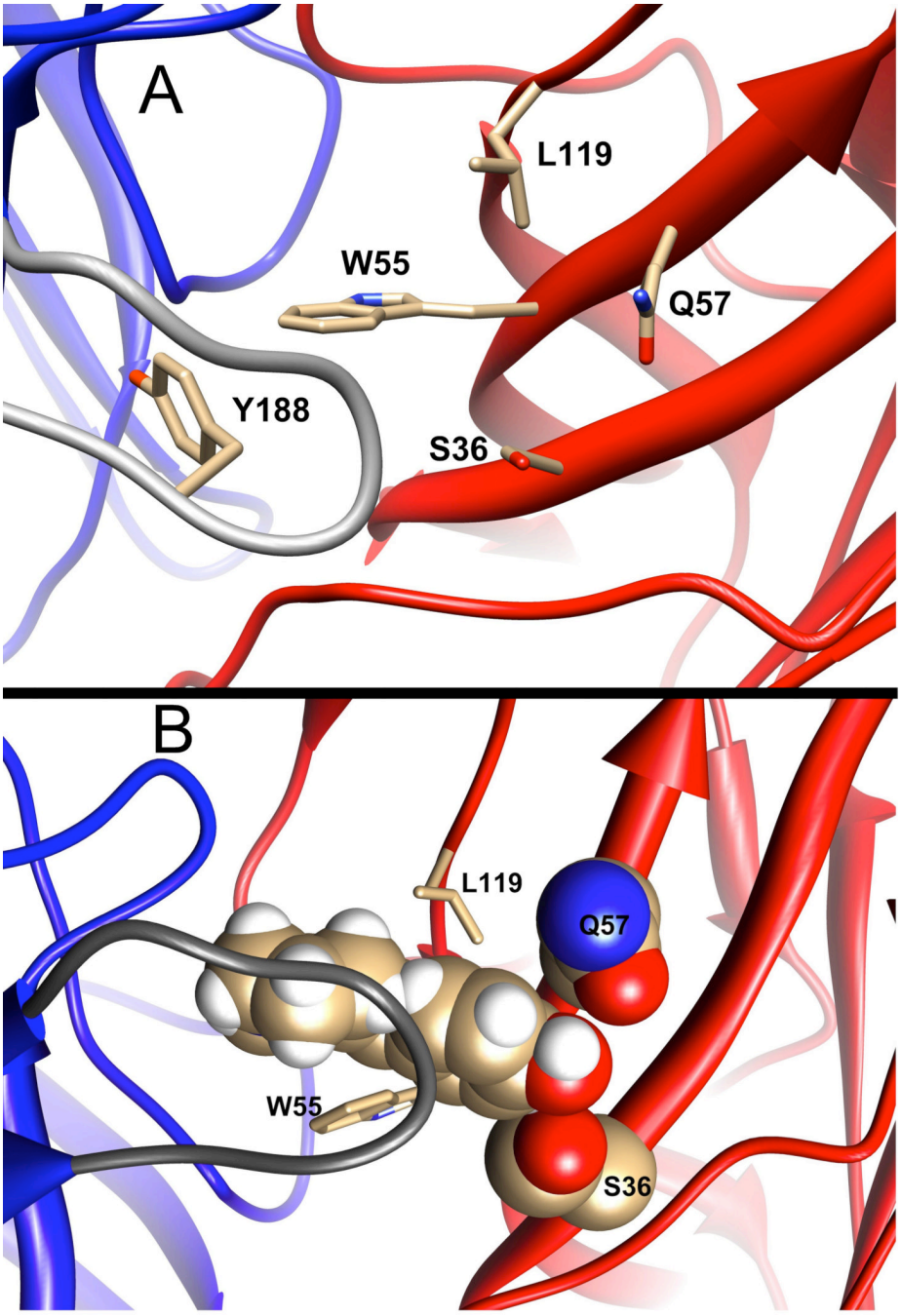

Figure 2. α7 nAChR BA binding site modeling

A) The agonist binding site for the α7 nAChR, displaying several of the residues which have been documented to influence agonist binding and/or the conformational transitions that follow binding [16, 33, 34]. **B)** The best docked pose for 4OHBA in the putative agonist binding site of an α7 homology model. The 4OH group is nestled between S36 and Q57.

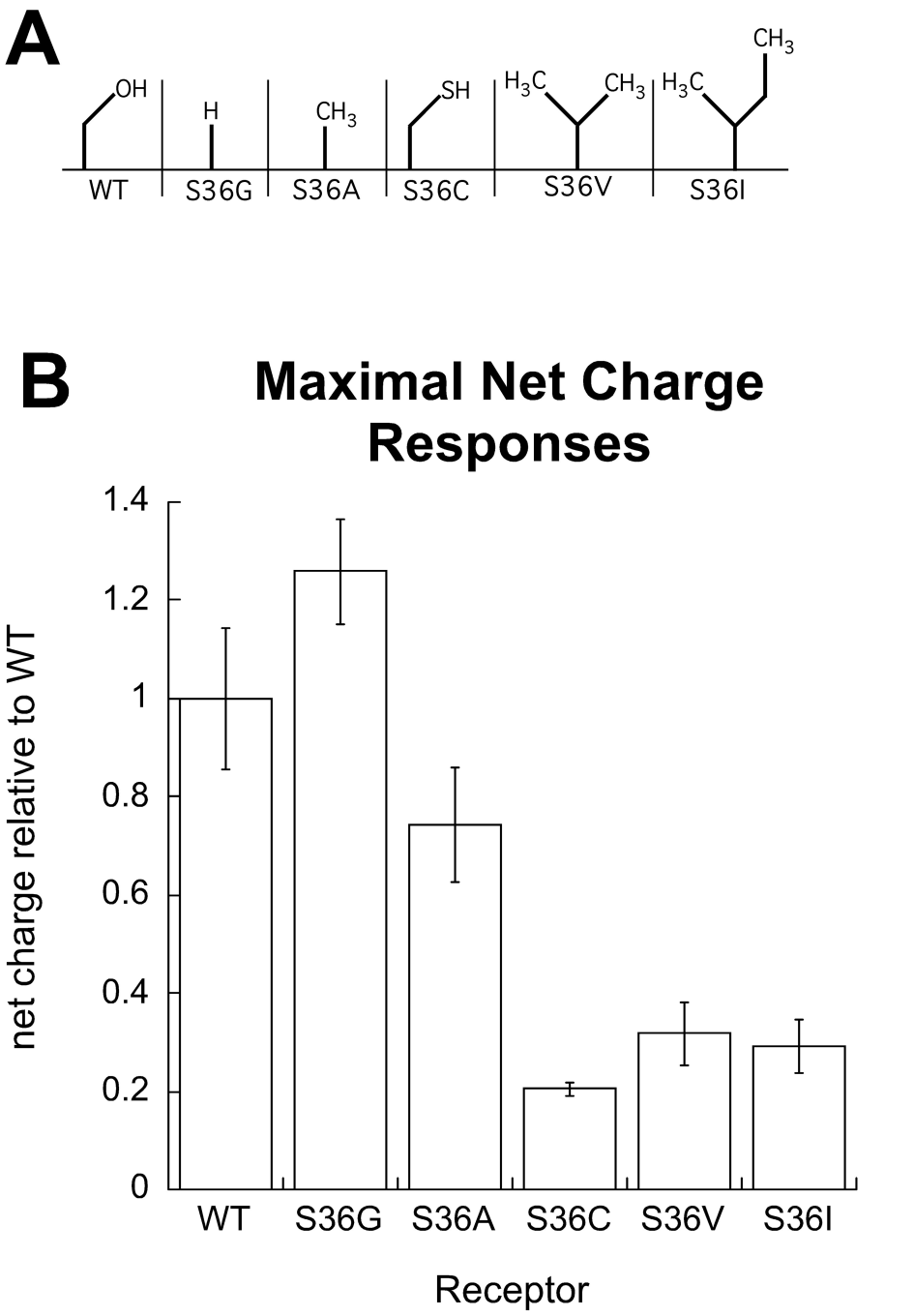

Figure 3. Structure and ACh responsiveness of α7 nAChR mutants

A) Molecular structure of WT (hydrophilic) and mutant (hydrophobic) residue side groups. **B**) Maximum response comparison between WT α7 and mutants. Mutant residues are roughly arranged left to right in order of increasing size of their hydrophobic side group. Each oocyte was injected with equal amounts of cRNA and given equal amounts of time to express. Net charge was recorded during 3mM ACh applications, with each response shown as the average of at least four recordings on separate oocytes. Error bars represent standard errors (S.E.M.) between the multiple recordings. All average responses were normalized to the average WT response recorded on the same day.

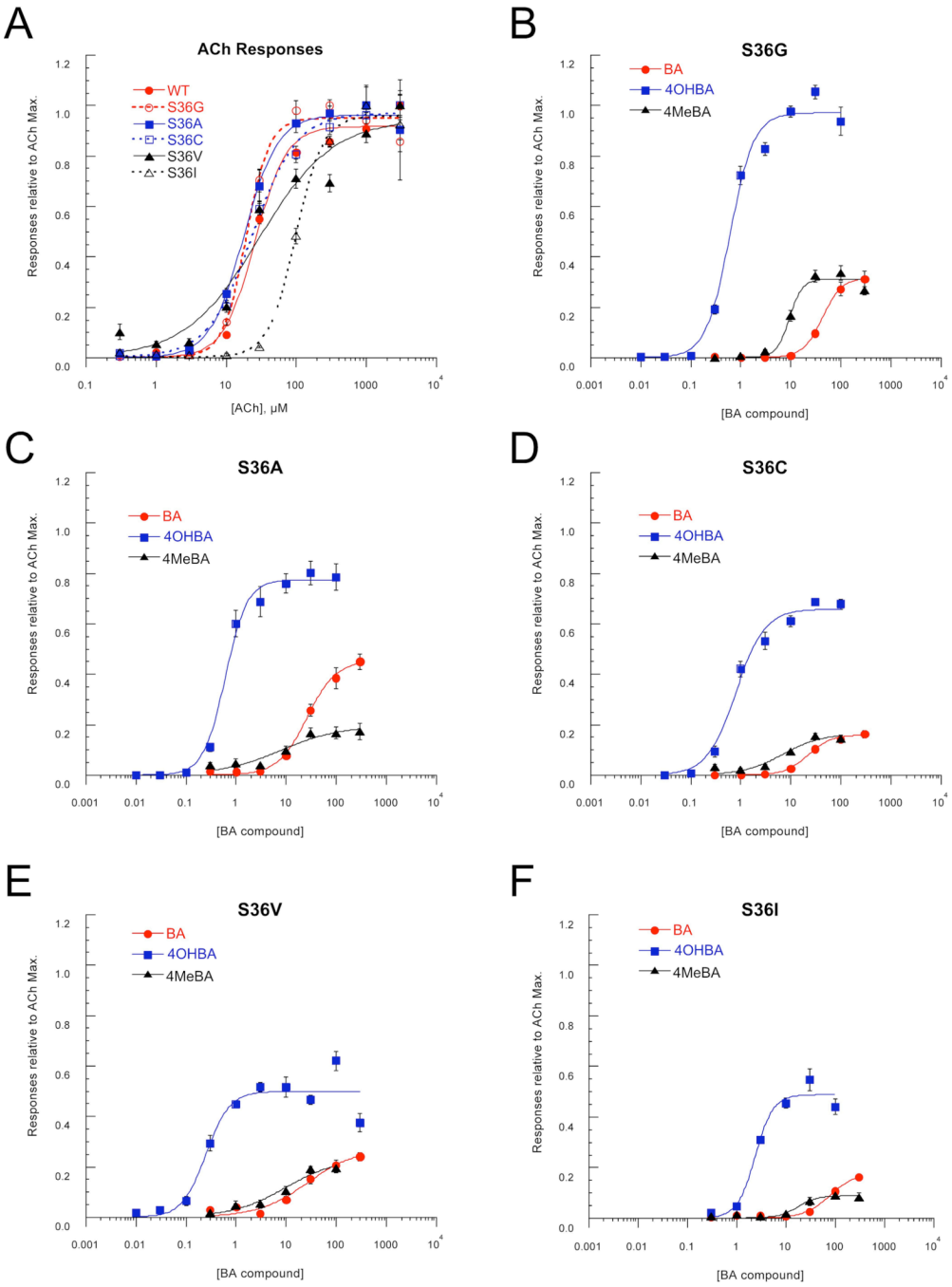

Figure 4. Effects of benzylidene anabaseines on α7 nAChR mutants

A) The concentration dependence of the ACh-evoked net charge responses for the WT α7 receptor and all mutants. Nearly equivalent ACh potency for all receptors was observed, except for the S36I mutant. **B–F)** Net charge CRCs for BA, 4OHBA, and 4MeBA on **B**) S36G, **C**) S36A, **D**) S36C, **E**) S36V, and **F**) S36I. All points are the averages ± SEM for at least four cells. The data in panel A are normalized to the maximal ACh responses for each receptor subtype. The data for the BA compounds (panels B–F) are expressed relative to the ACh maximal responses of the respective subtypes.

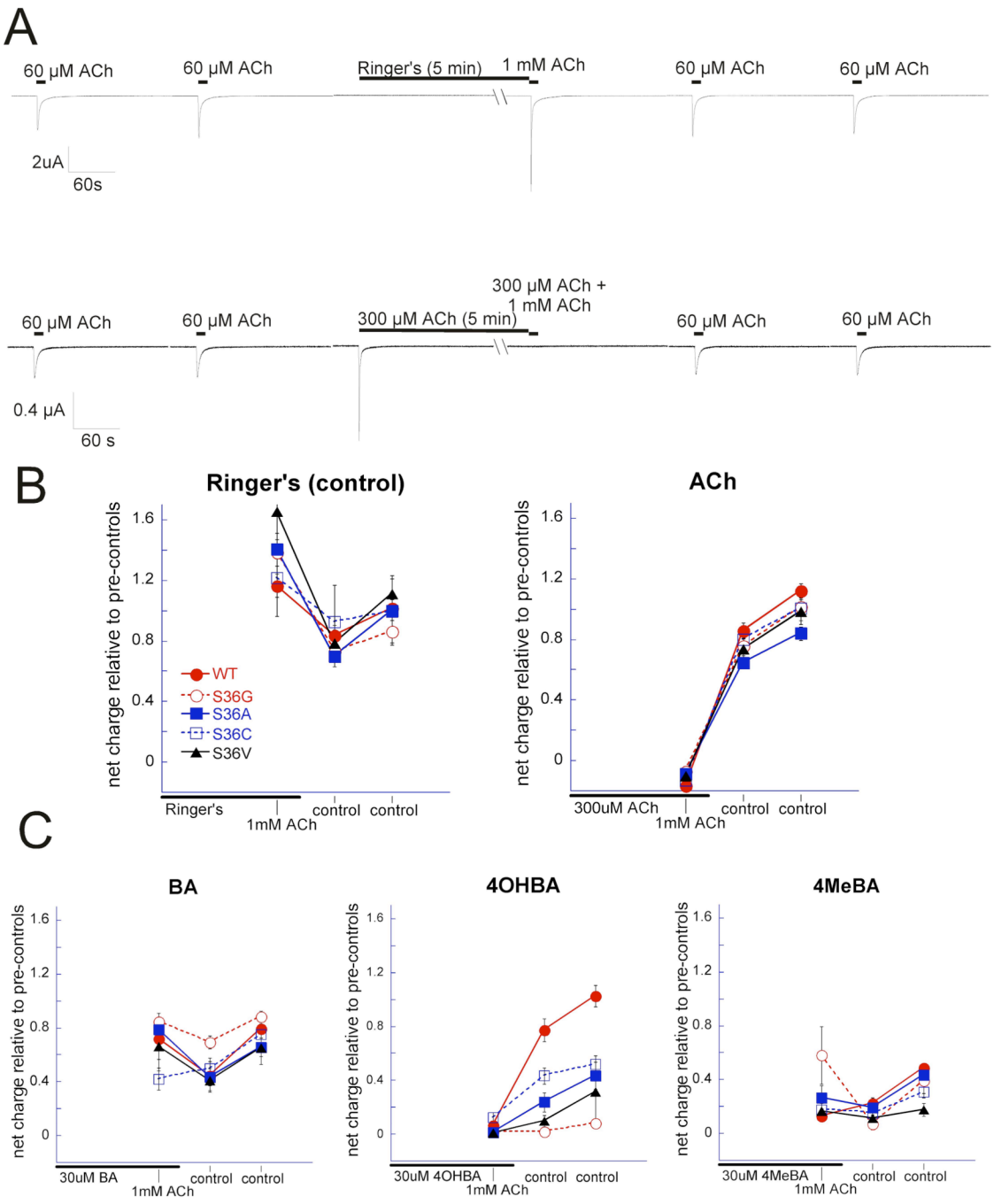

Figure 5. Induction of RD

A) Representative sample raw data traces illustrating the protocol used to determine the desensitization produced by pre-incubations with ACh or BA compound, compared to Ringer's controls (topmost traces). After 5-minute Ringer's control incubation, the application of 1 mM ACh produced a large response (left plot in panel B). In contrast, after a 5-minute pre-incubation with 300 μM ACh, the addition of 1 mM ACh produced no further response (lower traces and right plot in panel B). The two post-treatment control ACh applications (separated by 3 min) showed little to no significant RD in either trace, as expected. **B**) The average data for each of the receptor subtypes with the protocols illustrated

in Panel A. The post-treatment control ACh applications are indicated as "control" on the abscissa of the plots. **C)** Results obtained when the cells were pre-incubated with 30 μM of the BA compounds. The data in B & C are the averages ± SEM for at least four cells in each condition. Data for each cell were calculated relative to the average net charge response to two initial ACh controls, as shown in panel A.

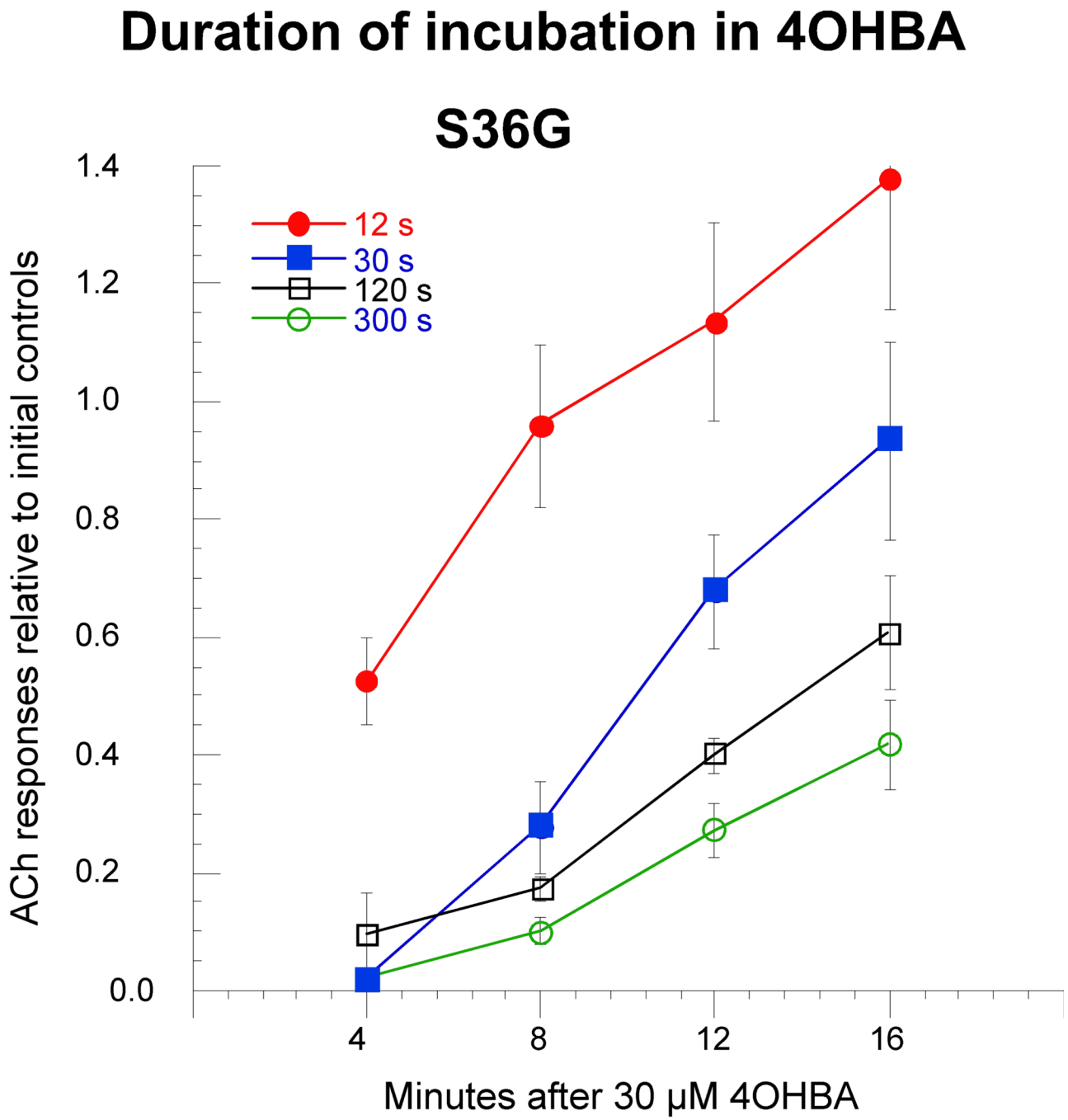

Figure 6. Duration of 4OHBA exposure affects extent of desensitization

Recovery of ACh control responses of S36G receptors following incubations in 30 μM 4OHBA for varying durations. The data are the averages ± SEM for at least four cells in each condition.

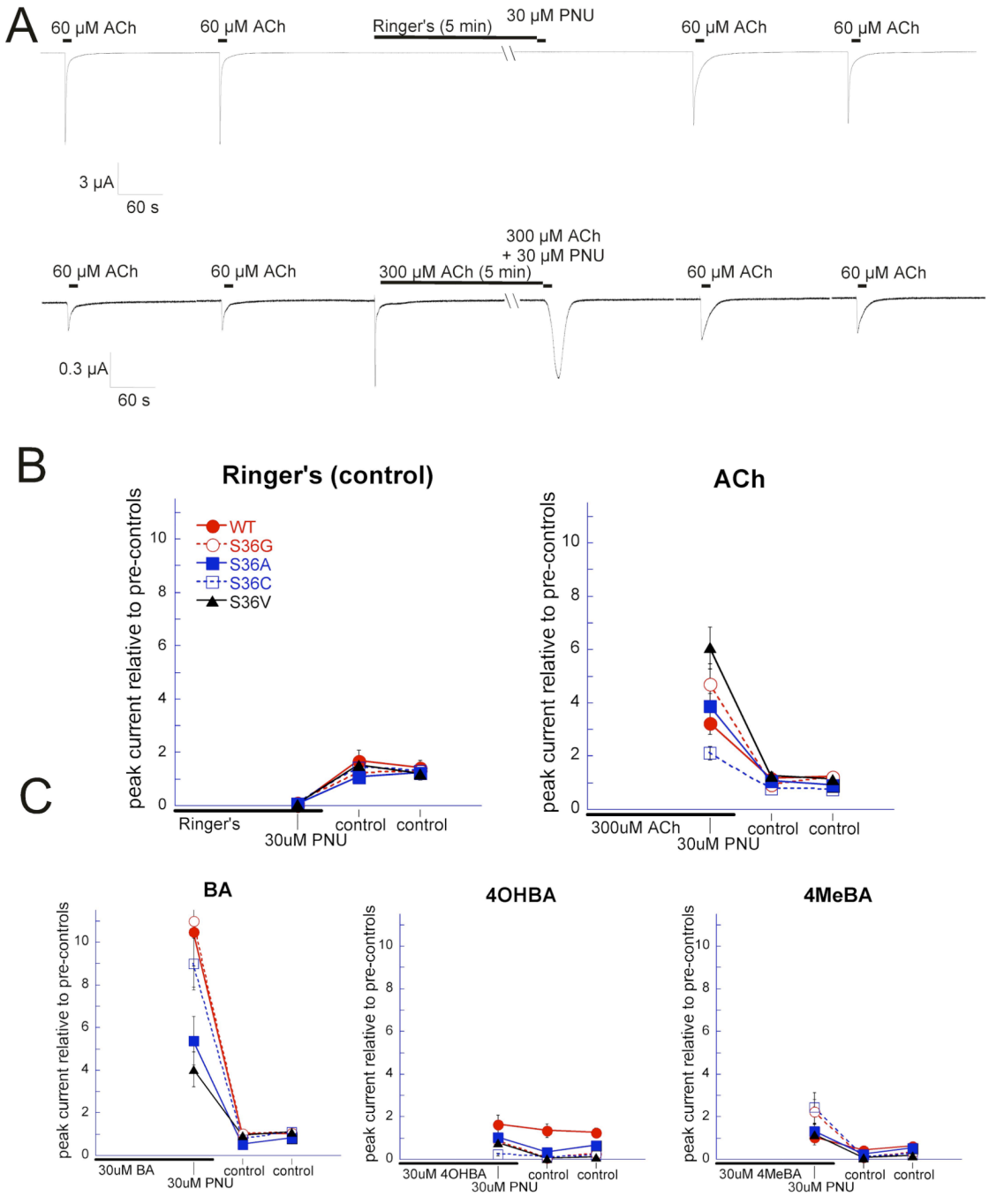

Figure 7. Induction of D_S

A) Representative sample raw data traces illustrating the protocol used and the Ringer's and ACh controls. After 5-minute pre-incubation with 300 μM ACh (lower trace) but not with Ringer's (upper trace), the application of 30 μM PNU-120596 produced large responses that varied depending on the agonist and receptor subtype. **B**) The average data for each of the receptor subtypes with the protocols illustrated in Panel A with either Ringer's or ACh preincubations. The post-treatment control ACh applications are indicated as "control" on the abscissa of the plots. **C)** Results obtained when the cells were pre-incubated with the 30 μM of the BA compounds. The data in B & C are the averages ± SEM for at least four cells

in each condition. Data for each cell were calculated relative to the average net charge response to two initial ACh controls.

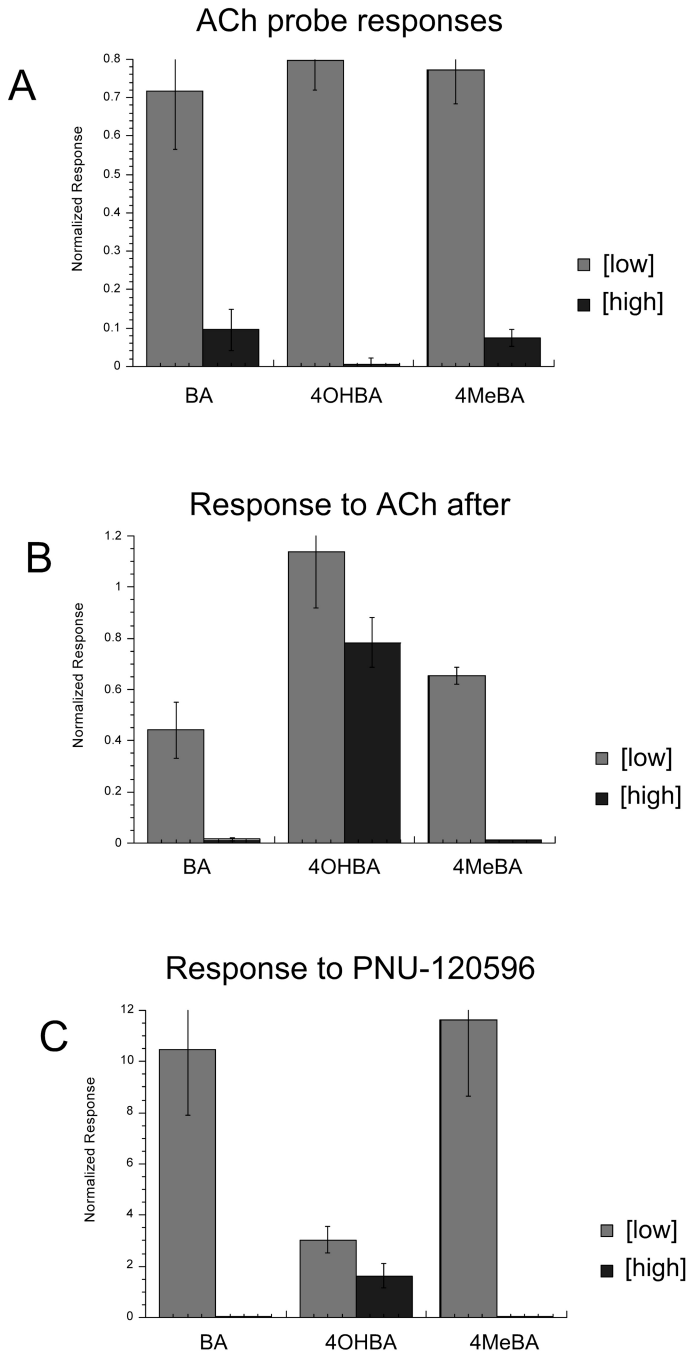

Figure 8. Effects of binding-site saturation on desensitization

Effects of BA concentrations on the pre-incubation effects on desensitization (A), RD (B), or the induction of Ds (C). Experiments were conducted using the protocols illustrated in Figures 5 and 7 with WT α7 receptors with drug concentrations both lower and higher than their respective EC_{50}s (BA: EC_{50}=40μM, Low=30μM, High=300μM; 4OHBA: EC_{50}=6μM, Low=3μM, High=30μM; 4MeBA: EC_{50}=30μM, Low=10μM, High=100μM). **A)** Levels of activation by 1mM ACh immediately after a 5-minute bath application of each BA compound at both high and low concentrations (protocol illustrated in Figure 5). As expected, ACh-evoked responses were higher after the low concentration-evoked response

than after the high concentration incubations. **B)** Levels of activation by control ACh applications after complete washout of each drug bath (see representative data in Figure 5A). Responses significantly smaller than 1 are indicative of RD. RD was most evident after pre-incubations with high concentrations of the more hydrophobic BA compounds. **C)** Responses to application of PNU-120596 immediately following drug baths (as illustrated in Figure 7). Responses to PNU-120596 by desensitized receptors are indicative of the D_s state. The data are the averages ± SEM for at least four cells in each condition. Normalized data for each cell were calculated relative to the average net charge response to two initial ACh controls.

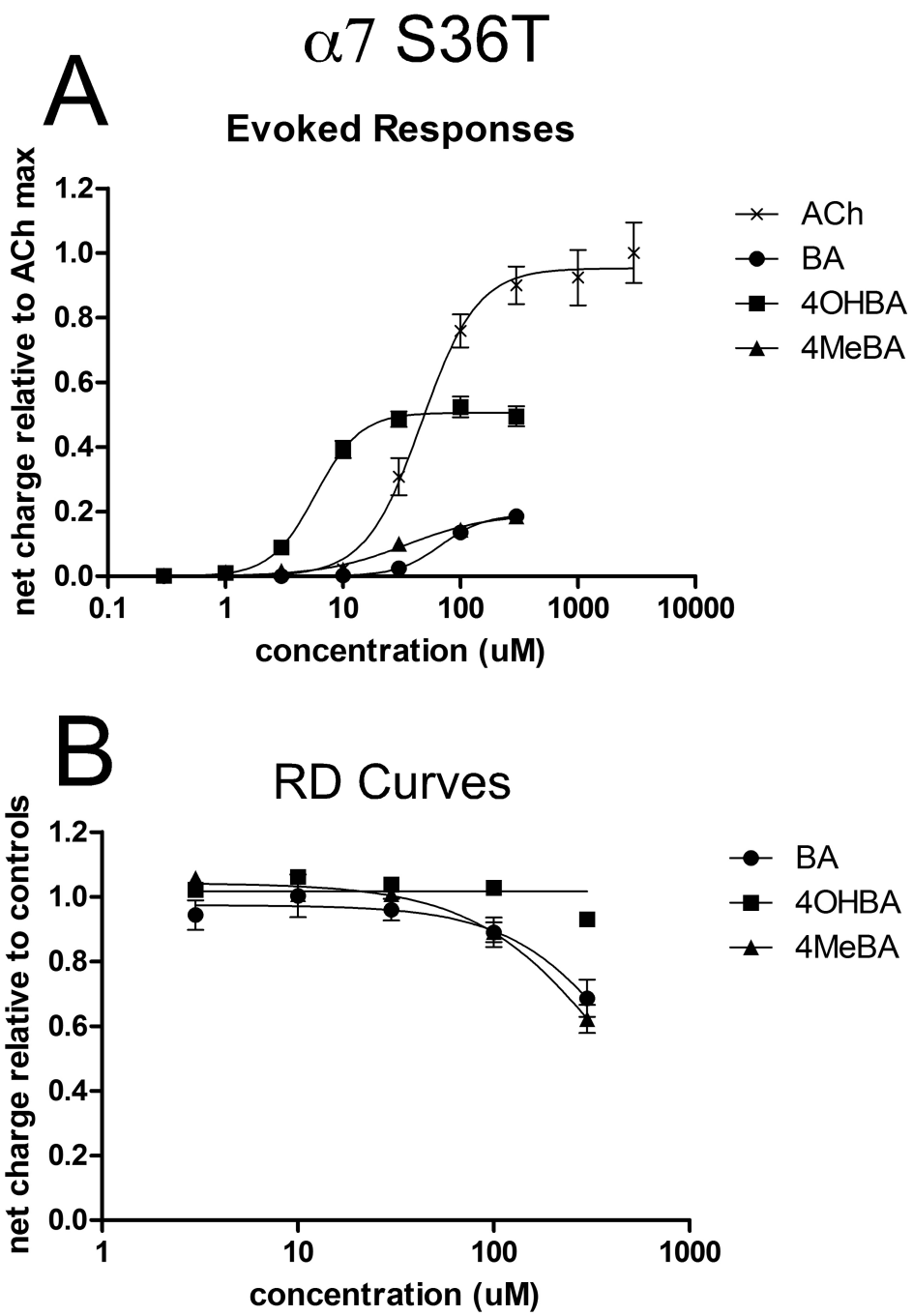

Figure 9. BA's effects on the α7 S36T mutant

A) CRCs for ACh, BA, 4OHBA, and 4MeBA on the α7 S36T mutant receptor. Points were generated by calculating the area of each test response relative to the response by the preceding ACh control and then normalized to the maximal ACh response, observed at 3mM ACh. **B**) RD curves for BA, 4OHBA, and 4MeBA on S36T. Points were generated by calculating the area of each control response immediately following a test application relative to the control response preceding that application.

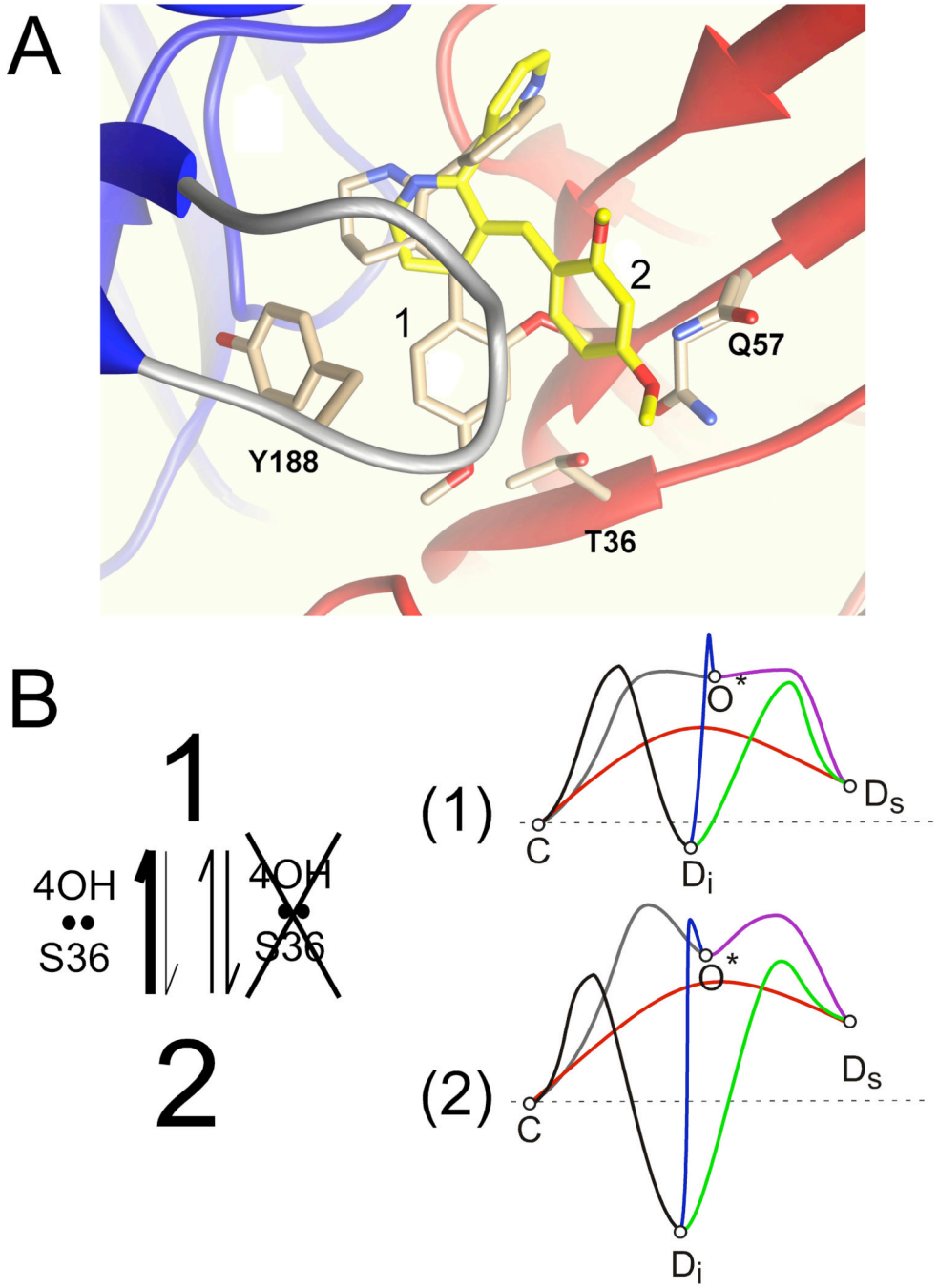

Figure 10. BA-induced conformational states of the α7 nAChR

A) Two unique binding orientations for *Aplysia* AChBP fully occupied with GTS-21 (2,4DiMeOBA), observed through x-ray crystallography as extrapolated from PDB ID 2WNJ (Hibbs et al., 2009). **B**) Proposed relationship between S36 H-bonding and the relative stability of the two binding orientations observed for GTS-21 and the hypothetical energy landscapes for the conformational transitions promoted by the two binding modes. Binding in the number 2 orientation, which is less likely to occur when there is an H-Bond interaction between a 4OHBA and S36, more effectively promotes RD and the induction of D_i.

Table 1

Summary of data for CRC curves for ACh and BA compounds on all receptors. I_{max} represents the maximal response on the CRC curve relative to the maximal response from ACh and is used as a measure of relative drug efficacy. I_{max} is set to 1 for ACh on all receptors. EC_{50} values are in units of μM, and are used as a measurement of potency for agonism. Parenthetical values indicate the measurement's error estimated from the curve fit to the average data over the concentration range of 300 nM–300 μM.

	ACh		BA		4OHBA		4MeBA	
	EC_{50} (μM)	I_{max}	EC_{50} (μM)	I_{max}	EC_{50} (μM)	I_{max}	EC_{50} (μM)	
WT	26(3)	0.31(0.01)	39(3)	0.385(0.006)	5.5(0.3)	0.14(0.01)	29(3)	
S36G	16(2)	0.316(0.003)	44(1)	0.89(0.06)	0.53(0.15)	0.31(0.02)	9.5(1.2)	
S36A	18(1.2)	0.45(0.02)	27(3)	0.73(0.03)	0.57(0.09)	0.19(0.04)	7.9(6.4)	
S36C	24(2)	0.30(0.01)	22(2)	0.63(0.02)	0.75(0.12)	0.14(0.02)	5.5(2.4	
S36V	28(12)	0.27(0.05)	27(17)	0.50(0.03)	0.25(0.07)	0.15(0.04)	3.5(3.4)	
S36I	100(6)	0.18(0.02)	81(15)	0.46(0.03)	2.3(0.5)	0.088(0.007)	17.6(3.7)	
S36T	47(5)	0.19(0.01)	68(0.1)	0.50(0.01)	5.9(0.3)	0.19(0.02)	34(10)	

Table 2

Summary of data for RD curves for BA compounds on all receptors. IC_{50} values are in units of μM, and are used as a measurement of potency for producing long-lasting desensitization. Parenthetical values indicate the measurement's error estimated from the curve fit to the average data over the concentration range of 300 nM–300μM. Values labeled NA were calculated to be significantly larger than 300 μM and thus clearly out of range of the concentrations studied in these experiments.

	BA	4OHBA	4MeBA
	IC_{50} (μM)	**IC_{50} (μM)**	**IC_{50} (μM)**
WT	270(53)	NA	110(30)
S36G	357(27)	134(20)	51(20)
S36A	91(11)	203(49)	145(46)
S36C	189(64)	233(25)	52(8)
S36V	217(51)	61(40)	91(25)
S36I	NA	NA	153(14)
S36T	720(126)	NA	450(45)